

## TWO PROTON EMISSION WITH ELECTROMAGNETIC PROBES

A.M. Lallena,<sup>1,\*</sup> M. Anguiano,<sup>2,†</sup> and G. Co<sup>3,‡</sup>

<sup>1</sup>*Departamento de Física Moderna, Universidad de Granada, E-18071 Granada, Spain.*

<sup>2</sup>*Departamento de Radiación Electromagnética, Instituto de Física Aplicada, CSIC,  
c/ Serrano 144, E-28006 Madrid, Spain.*

<sup>3</sup>*Dipartimento di Fisica Università di Lecce and I.N.F.N Sez. di Lecce,  
I-73100 Lecce, Italy*

A model to study two-proton emission from nuclei induced by electromagnetic probes is developed. The process is due to one-body electromagnetic operators, acting together with short-range correlations, and two-body  $\Delta$  currents. The model includes all the diagrams containing a single correlation function. The sensitivity of the cross section to the details of the correlation function is studied by using realistic and schematic correlations. Results for the  $^{16}\text{O}$  nucleus are presented.

### 1. INTRODUCTION

In this work we apply the model we have developed in these last years [1]-[4] to describe electromagnetic responses by considering also short-range correlations (SRC) to the case of the electromagnetically induced two-nucleon knockout from nuclei. The aim of our model is to take into account the SRC in electromagnetic processes involving nuclei with  $A > 4$ , in such a way that different processes, like inclusive electron scattering, one- and two-nucleon emission induced by electron scattering and, eventually, real photon scattering, can be described by using the same methodology. The idea was to have a consistent view of the different processes.

The linear response of the nucleus to an external operator  $O(\mathbf{q})$  can be written as:

$$S(\mathbf{q}, \omega) = -\frac{1}{\pi} \text{Im} D(\mathbf{q}, \omega),$$

with

$$D(\mathbf{q}, \omega) = \sum_n \xi_n^+(\mathbf{q}) (E_n - E_0 - \omega + i\eta)^{-1} \xi_n(\mathbf{q})$$

where we have defined

$$\xi_n(\mathbf{q}) = \frac{\langle \Psi_n | O(\mathbf{q}) | \Psi_0 \rangle}{\langle \Psi_n | \Psi_n \rangle^{\frac{1}{2}} \langle \Psi_0 | \Psi_0 \rangle^{\frac{1}{2}}}$$

This function involves the transition matrix element between the initial and the final states of the nucleus. These states are construct by acting with a correlation operator  $F$  on uncorrelated Slater determinants, as established by the Correlated Basis Function theory:

$$|\Psi_0\rangle = F |\Phi_0\rangle \quad |\Psi_n\rangle = F |\Phi_n\rangle.$$

---

\*Electronic address: lallena@ugr.es

†Electronic address: marta.anguiano@iec.csic.es

‡Electronic address: Giampaolo.Co@le.infn.it

Then the quantity  $\xi$  can be written as

$$\xi_n(\mathbf{q}) = \frac{\langle \Phi_n | F^+ O(\mathbf{q}) F | \Phi_0 \rangle}{\langle \Phi_0 | F^+ F | \Phi_0 \rangle} \left[ \frac{\langle \Phi_0 | F^+ F | \Phi_0 \rangle}{\langle \Phi_n | F^+ F | \Phi_n \rangle} \right]^{\frac{1}{2}}.$$

We consider scalar correlation functions of the type:

$$F = \prod_{i < j} f_{ij},$$

therefore the  $\xi$  function results

$$\xi_n(\mathbf{q}) = \frac{\langle \Phi_n | O(\mathbf{q}) \prod_{i < j} (1 + h_{ij}) | \Phi_0 \rangle}{\langle \Phi_0 | \prod_{i < j} (1 + h_{ij}) | \Phi_0 \rangle} \left[ \frac{\langle \Phi_0 | \prod_{i < j} (1 + h_{ij}) | \Phi_0 \rangle}{\langle \Phi_n | \prod_{i < j} (1 + h_{ij}) | \Phi_n \rangle} \right]^{\frac{1}{2}},$$

where the  $h$  function is defined as:

$$h_{ij} = f_{ij}^2 - 1.$$

We perform the full cluster expansion of this expression and this allows us to eliminate the unlinked diagrams. At this point we insert the main approximation of our model by truncating resulting expansion such as only those diagrams which involve a single correlation function  $h$  are retained:

$$\xi_n(\mathbf{q}) \rightarrow \xi_n^1(\mathbf{q}) = \langle \Phi_n | O(\mathbf{q}) \left( 1 + \sum_{i < j} h_{ij} \right) | \Phi_0 \rangle_L.$$

In the above expression the subscript  $L$  indicates that only linked diagrams are included in the expansion.

For one-particle one-hole final states, the function  $\xi$  includes three terms:

$$\xi_{1p1h}^1(\mathbf{q}) = \langle \Phi_{1p1h} | O(\mathbf{q}) | \Phi_0 \rangle + \langle \Phi_{1p1h} | O(\mathbf{q}) \sum_{j > 1}^A h_{1j} | \Phi_0 \rangle + \langle \Phi_{1p1h} | O(\mathbf{q}) \sum_{1 < i < j}^A h_{ij} | \Phi_0 \rangle$$

The contributions of the various terms of the above expression are shown in Fig. 1 in terms Meyer-like diagrams. In addition to the uncorrelated transition represented by the one-point diagram (1.1). But, besides, also 4 two-point diagrams and 6 three-point diagrams are present. These new terms are necessary to get a proper normalization of the nuclear wave functions. In the figure, the black squares represent the points where the external operator is acting, the dashed lines represent the correlation function  $h$  and the continuous oriented lines represent the single-particle wave functions. The letters  $h$ ,  $i$  and  $k$  label holes, while  $p$  labels a particle. A sum over  $i$  and  $k$  is understood.

Our model was tested by comparing our nuclear matter charge response functions with those obtained by considering the full cluster expansion [6]. As we can see in Fig. 2 both calculations overlap and this gave us confidence to extend the model to other situations.

With this model we have analyzed different processes involving both real and virtual photons. Inclusive (e,e') excitation of discrete nuclear states showed a very small effect due to SRC [1]. On the other hand, inclusive electron scattering in the quasi-elastic peak region presented SRC contributions smaller than final state interactions effects [2]. These last also dominate in the case

of (e,e'p) reactions [3]. Finally, in ( $\gamma$ ,p) we found a kinematic region showing pronounced sensitivity to the SRC. Unfortunately, in this region, the effect of meson exchange currents (MEC) is much larger than that of SRC [4].

In all these processes the uncorrelated one-body response dominates the cross sections. To get rid of this contribution one has to investigate two nucleon emission processes. In this case one deals with two-body operators which can be either one-body operators acting in correlated nuclear states or MEC. If, in addition, one chooses two-proton emission, MEC involving charged mesons do not contribute and the situation is, at least in principle, rather clean to investigate SRC effects.

In case one has two-particle two-hole final states, the function  $\xi$  includes two terms:

$$\xi_{2p2h}^1(\mathbf{q}) = \langle \Phi_{2p2h} | O(\mathbf{q}) \sum_{1 < j}^A h_{1j} | \Phi_0 \rangle + \langle \Phi_{2p2h} | O(\mathbf{q}) \sum_{1 < i < j}^A h_{ij} | \Phi_0 \rangle$$

The first term (see Fig. 3) consists of 4 two-point diagrams. The second one results from the sum of 8 three-point diagrams. As in the previous case, this set of diagrams conserves the correct normalization.

The geometry of the two-proton emission process produced by electron scattering from nuclei is shown in Fig. 4. The cross section is given by:

$$\frac{d^8\sigma}{d\epsilon' d\Omega_e d\epsilon_1 d\Omega_{p_1} d\Omega_{p_2}} = \frac{m^2 |\mathbf{p}_1| |\mathbf{p}_2|}{(2\pi)^6} \sigma_{\text{Mott}} f_{\text{rec}} (v_l w_l + v_t w_t + v_{tl} w_{tl} + v_{tt} w_{tt}) ,$$

where  $\epsilon'$  is the energy of the outgoing electron,  $\Omega_e$  is the solid angle of its direction,  $\epsilon_1$  is the energy of the one emitted proton,  $\Omega_{p_1}$  and  $\Omega_{p_2}$  are the solid angles of the directions of the two emitted protons,  $\mathbf{p}_1$  and  $\mathbf{p}_2$  are their momenta,  $m$  is the proton mass,  $\sigma_{\text{Mott}}$  is the Mott cross section and  $f_{\text{rec}}$  describes the recoil of the residual nucleus. The  $v$ 's are kinematic factors, while the  $w$  responses include the information about the nuclear structure and are given in terms of matrix elements of the charge and current operators.

In our calculations we have considered the charge and the magnetization current one-body operators and the  $\Delta$ -isobar two-body current, specifically these terms proportional to  $\tau_3$  [5].

The hole wave functions have been obtained from a Woods-Saxon potential whose parameters have been fixed to reproduce rms charge radii and single particle energies around the Fermi energy, while for the particles wave functions we used the optical potential of Schwandt *et al.* [7].

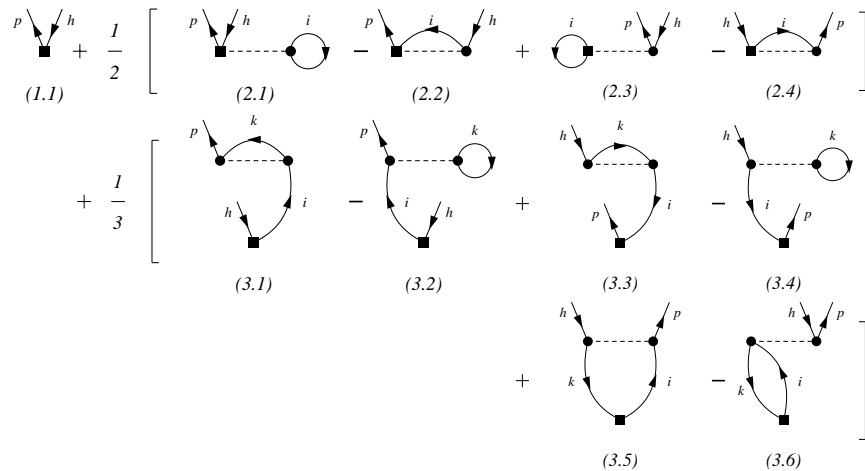


FIG. 1: Meyer-like diagrams contributing to  $\xi_{1p1h}^1(\mathbf{q})$ .

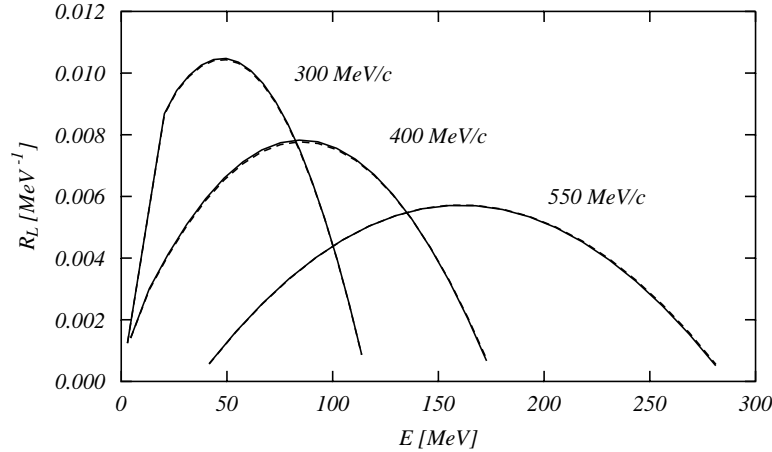


FIG. 2: Nuclear matter one-particle one-hole longitudinal response calculated with our model (full lines) and with FHNC (dashed lines)

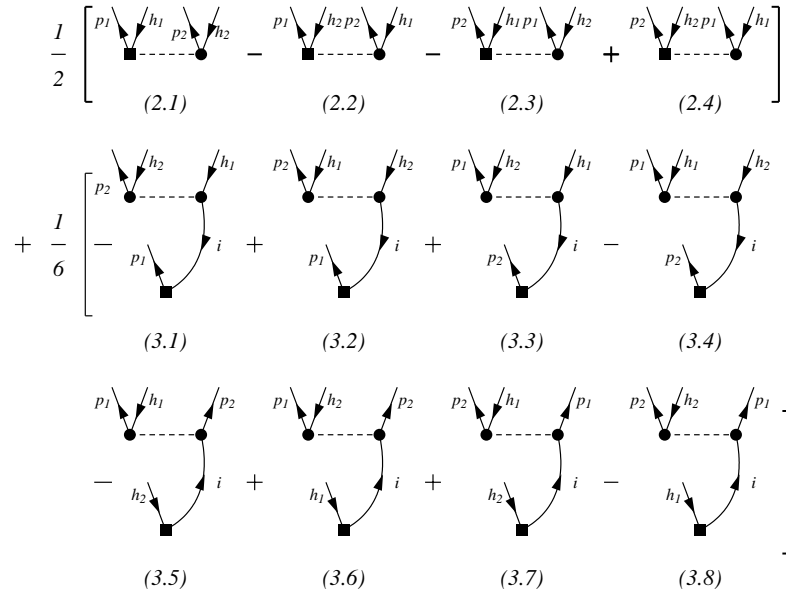


FIG. 3: Meyer-like diagrams contributing to  $\xi_{2p2h}^1(\mathbf{q})$ .

## 2. RESULTS

The particular aspect we have investigated concerns to the sensitivity of the (e,e'2p) cross section to the details of the SRC. This has been done by using the three correlation functions shown in Fig. 5. The G (Gaussian) and S3 correlations, have been taken from a FHNC calculation

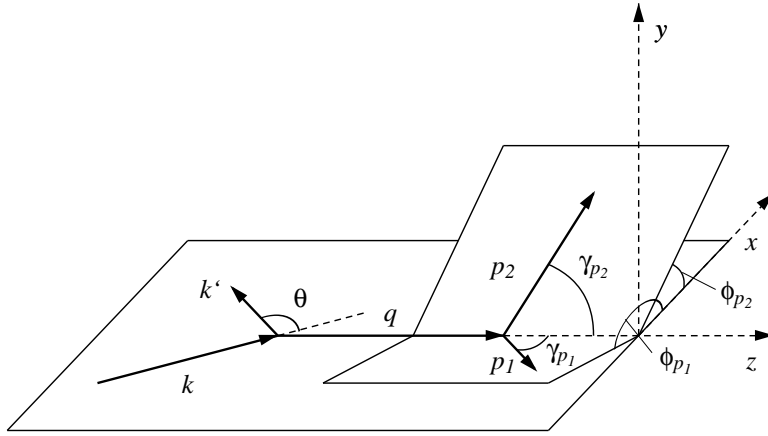


FIG. 4: Geometry of the (e, e' 2p) process.

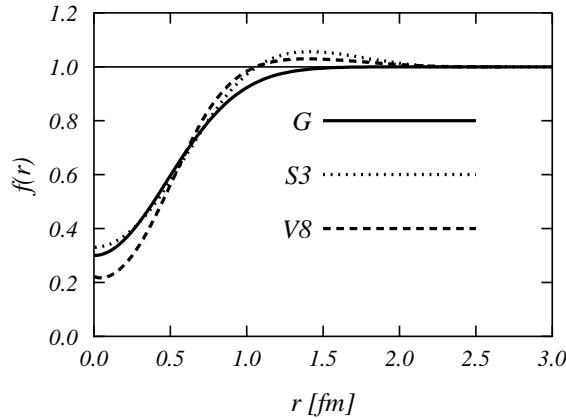


FIG. 5: Correlation functions used in our calculations.

done with semi-realistic interaction [8]. The V8 correlation is the scalar part of a state dependent correlation used in FHNC calculation done with a V8' Argonne interaction plus three-body Urbana IX interaction [9].

The minimum of the G and S3 interaction is almost the same, while the V8 interaction has a deeper value. The V8 and S3 correlations overshoot the asymptotic value of 1 in the region between  $r=1$  and  $2$  fm. The cross sections obtained with these correlations for  $^{16}\text{O}$  are shown in Fig. 6. Apart the result of the  $1^+$  state dominated by the two-body currents, all the other results have common trends. First, one should notice that the use of different correlations does not change the shape of the angular distribution. Second, the cross sections obtained with the Gaussian correlation, are larger than the other ones.

To understand this result, we have done a set of calculations with rather schematic correlations. These correlations are shown in the lower right panel of Fig. 7. The cross sections calculated with these correlations are shown in the other panels by lines of the same type. In these calculations the two-body  $\Delta$  currents have not been included.

The box correlation indicated by the full line is our reference correlation. Lowering the minimum (dashed lines) does not produce a large effect. The insertion of a part which overshoots the asymptotic value reduces the cross section (dotted lines). An analogous effect is obtained by reducing the size of the box (dashed-dotted lines).

These results can be understood by remembering that the quantity entering in the cross section calculation is  $h(r) = 1 - f^2(r)$ . The largest is the contribution of  $h$  to  $\xi_n^1(\mathbf{q})$ , the largest is the cross section. The overshooting of the asymptotic value, generates a term in  $h(r)$  of opposite sign with respect to the rest of the function, therefore the total contribution to the integral becomes smaller. The same effect can be obtained by reducing the size of the box as it is shown by the dashed dotted lines.

To finish, we show in Fig. 8 the effect of each of the three ingredients of the transition operator: the two- and three-point diagrams coming from the one-body charge and current operators and the  $\Delta$ -isobar current. As we can see, this last dominates the  $1^+$  results, while for the  $0_1^+$  the terms associated to SRC (in particular, these corresponding to 2-point diagrams) produce the larger contributions. In the case of the  $2_1^+$ , the 3-point diagrams are also relevant.

### 3. CONCLUSIONS

We have presented here results for the (e,e'2p) process in  $^{16}\text{O}$  and  $^{40}\text{Ca}$  obtained within a model which includes the effect of scalar SRC through diagrams with only one correlation line.

We have found that qualitative features, such as the shape of the angular distributions, are not sensitive to the details of the SRC. On the other hand, slight differences in the correlation function produce large modifications in the size of the cross sections.

However, the information about the SRC can be obtained only by a quantitative comparison between theoretical predictions and experimental data. Unfortunately the quantitative evaluation of the (e,e'2p) cross sections suffers from the uncertainties inherent to the required theoretical input.

These kind of experiments are not the unique tool to extract the characteristics of the SRC correlations, but another procedure allowing, together with elastic, inclusive and one-nucleon emission experiments, to obtain the information we are looking for. We are trying to describe all these process in a unique and coherent theoretical framework, thus permitting meaningful analysis of all of them.

---

- [1] S.R. Mokhtar, G. Co' and A.M. Lallena, Phys. Rev. C **62**, 067304 (2000).
- [2] G. Co' and A. M. Lallena, Ann. Phys. (N.Y.) **287**, 101 (2001).
- [3] S. R. Mokhtar, M. Anguiano, G. Co' and A. M. Lallena, Ann. Phys. (N.Y.) **292**, 67 (2001).
- [4] M. Anguiano, G. Co', A. M. Lallena and S.R. Mokhtar, Ann. Phys. (N.Y.) **296**, 235 (2002).
- [5] M. Anguiano, G. Co' and A. M. Lallena, J. Phys. G: Nucl. Part. Phys. **29**, 1 (2003).
- [6] J.E. Amaro, A.M. Lallena, G. Co' and A. Fabrocini, Phys. Rev. C **57**, 3473 (1998)
- [7] P. Schwandt *et al.*, Phys. Rev. C **26**, 55 (1982)
- [8] F. Arias de Saavedra, G. Co', A. Fabrocini and S. Fantoni, Nucl. Phys. A **605**, 359 (1996).
- [9] A. Fabrocini, F. Arias de Saavedra and G. Co', Phys. Rev. C **61**, 044302 (2000).

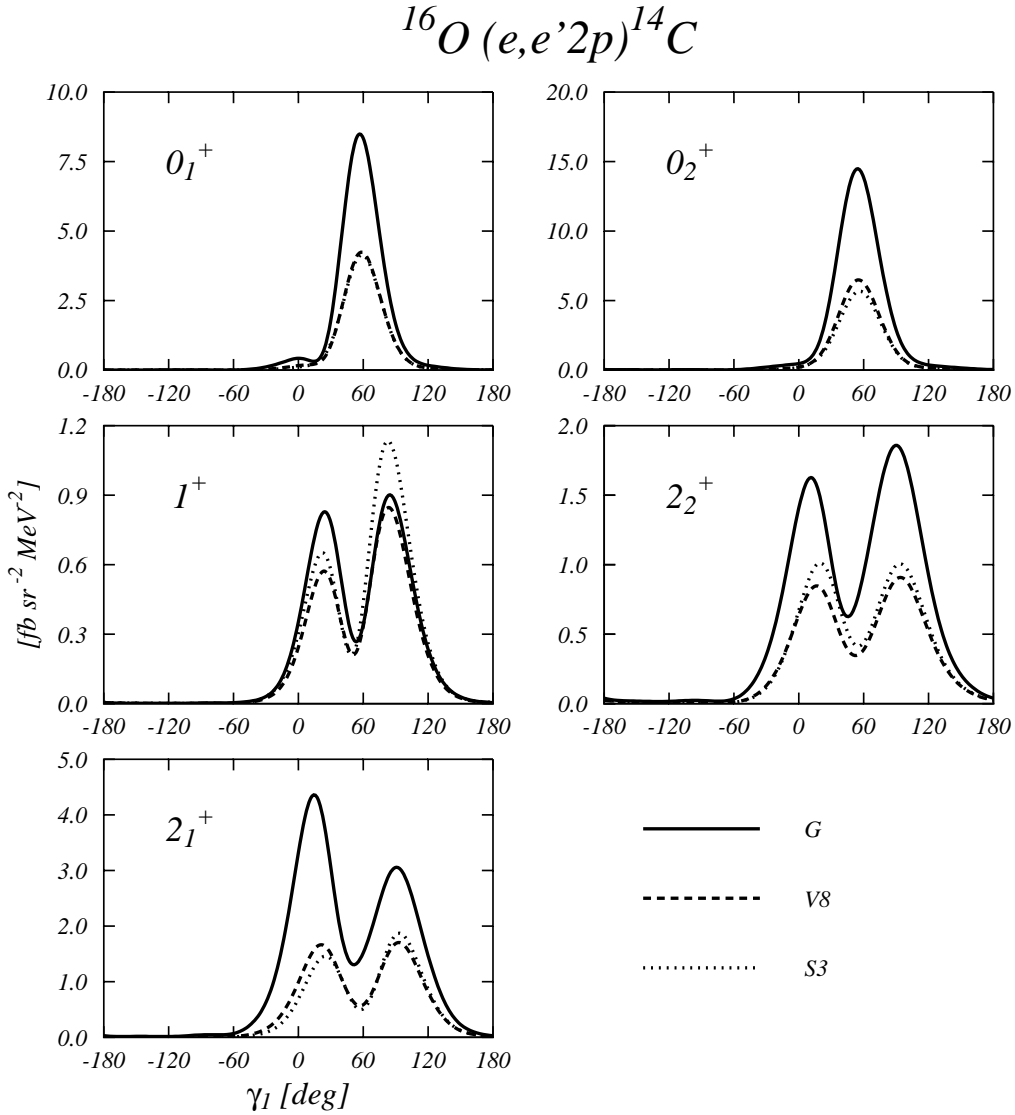


FIG. 6:  $^{16}\text{O}(e,e'2p)^{14}\text{C}$  cross sections calculated with the correlation functions shown in Fig. 5. The calculations have been performed for an electron incoming energy  $\epsilon = 800$  MeV, a momentum transfer  $q = 400$  MeV/c and a nucleus excitation energy  $\omega = 100$  MeV. The second proton was emitted with an energy  $\epsilon_2 = 40$  MeV and within an angle  $\gamma_{p_2} = 60^\circ$ . No recoil of the residual nucleus was considered and coplanar kinematics ( $\phi_{p_1} = \phi_{p_2} = 0$ ) was assumed. The angular momenta refer to the state of the residual nucleus:  $(1p_{1/2})^{-2} : 0_1^+$ ,  $(1p_{3/2})^{-2} : 0_2^+$ ,  $(1p_{1/2})^{-1}(1p_{3/2})^{-1} : 1^+$ ,  $(1p_{1/2})^{-1}(1p_{3/2})^{-1} : 2_1^+$  and  $(1p_{3/2})^{-2} : 2_2^+$

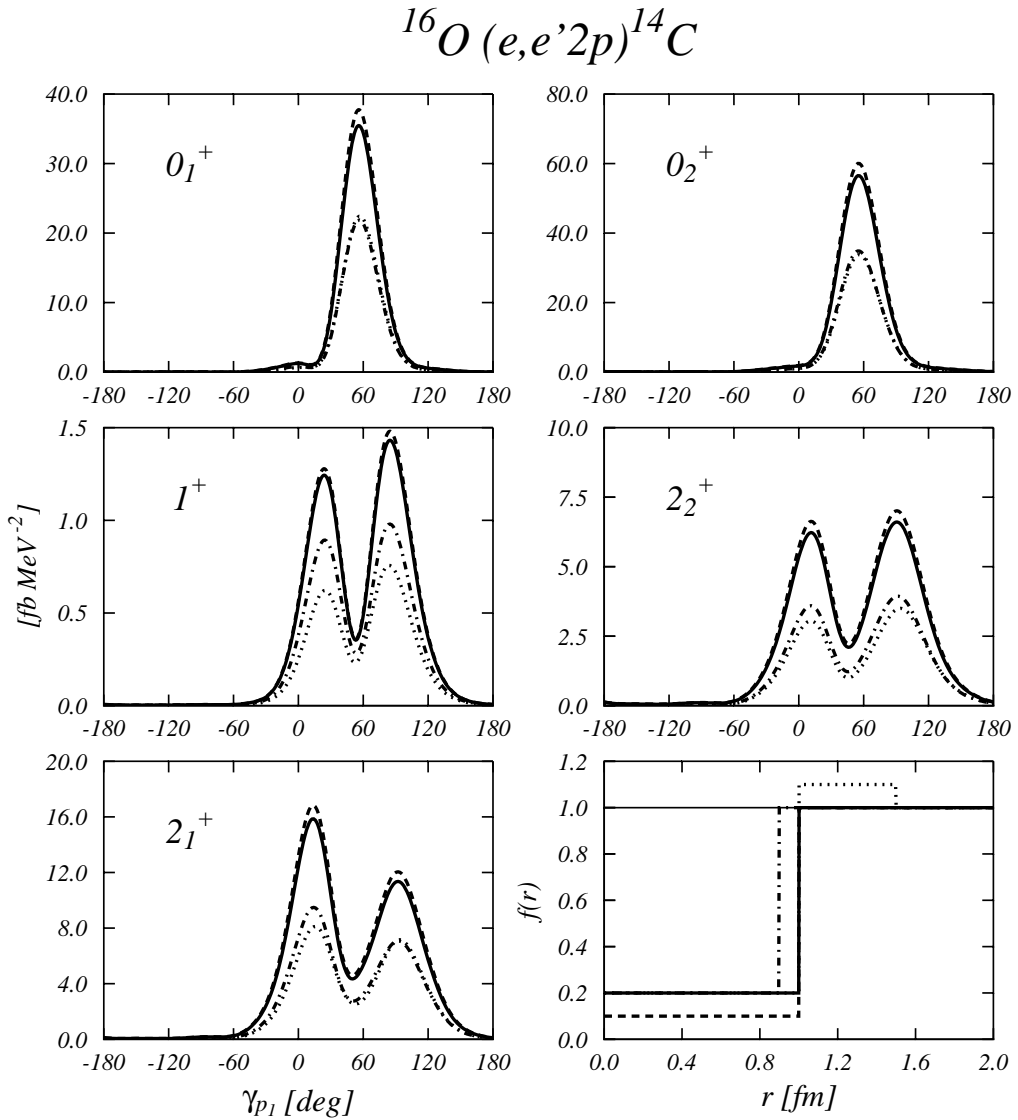


FIG. 7: Same as in Fig. 6 but for the schematic correlations shown in the lower right panel.

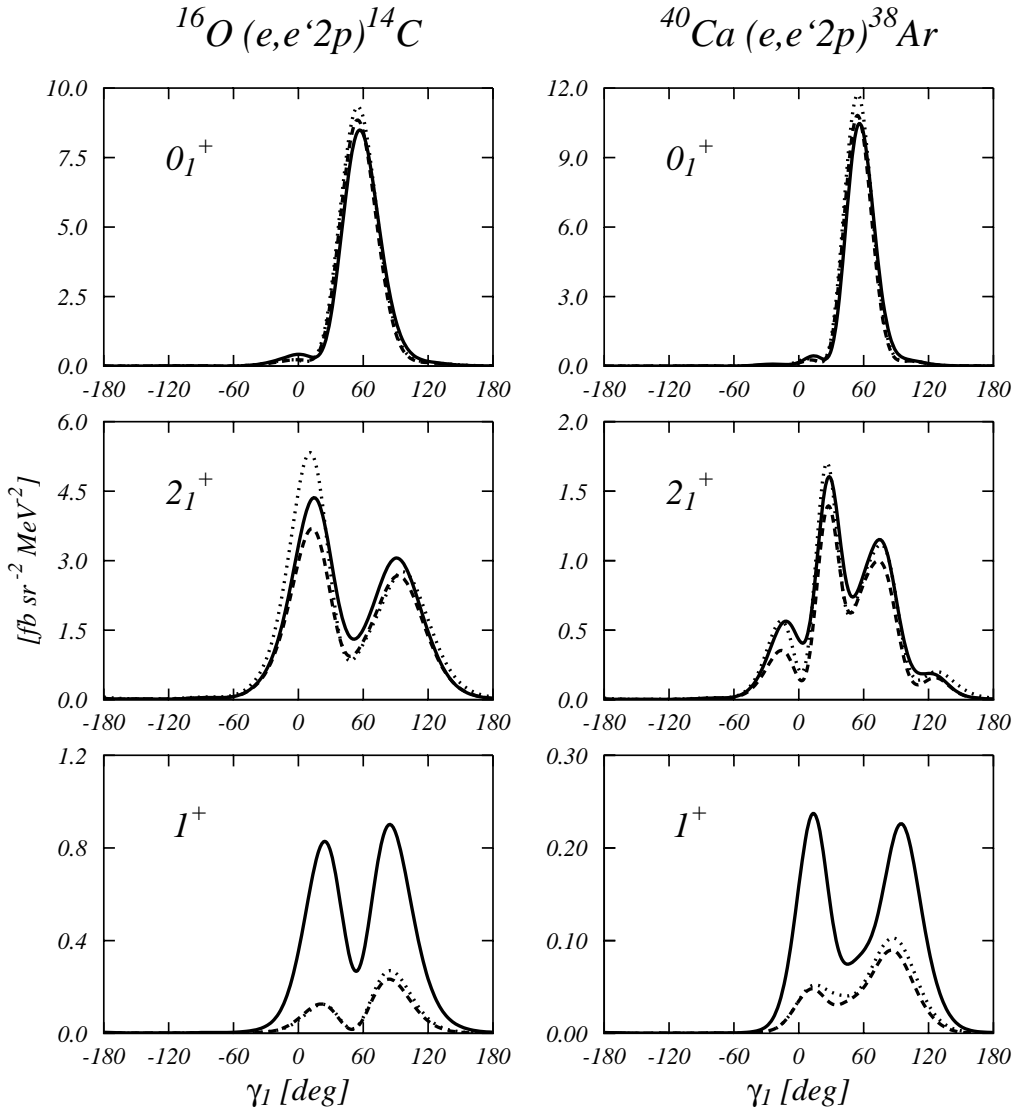


FIG. 8:  $^{16}\text{O}(\text{e},\text{e}'2\text{p})^{14}\text{C}$  and  $^{40}\text{Ca}(\text{e},\text{e}'2\text{p})^{38}\text{Ar}$  cross sections calculated with the same kinematics as in Fig. 6 and with the Gaussian correlation. Dotted curves include only the 2-point diagrams of Fig. 3. Dashed curves include also the 3-point of the same figure (except the last four which do not contribute to this process). Solid curves show the results when also the  $\Delta$  currents are included.